Applied Surface Science 438 (2018) 136–146

Contents lists available at ScienceDirect

Applied Surface Science

journal homepage: www.elsevier.com/locate/apsusc

Full Length Article

Induced superhydrophobic and antimicrobial character of zinc metal modified ceramic wall tile surfaces

Selçuk Özcan[a,*], Gökhan Açıkbaş[b], Nurcan Çalış Açıkbaş[c]

[a] Department of Chemical and Process Engineering, Bilecik Şeyh Edebali University, Bilecik 11210, Turkey
[b] Vocational School, Metallurgy Program, Bilecik Şeyh Edebali University, Bilecik 11210, Turkey
[c] Department of Metallurgy and Materials Engineering, Bilecik Şeyh Edebali University, Bilecik 11210, Turkey

ARTICLE INFO

Article history:
Received 18 April 2017
Received in revised form 22 June 2017
Accepted 1 August 2017
Available online 7 August 2017

Keywords:
Superhydrophobicity
Ceramic tile
Contact angle
Antimicrobial surface
Antimicrobial characterization
Ceramic glaze

ABSTRACT

Hydrophobic surfaces are also known to have antimicrobial effect by restricting the adherence of microorganisms. However, ceramic products are produced by high temperature processes resulting in a hydrophilic surface. In this study, an industrial ceramic wall tile glaze composition was modified by the inclusion of metallic zinc powder in the glaze suspension applied on the pre-sintered wall tile bodies by spraying. The glazed tiles were gloss fired at industrially applicable peak temperatures ranging from 980 °C to 1100 °C. The fired tile surfaces were coated with a commercial fluoropolymer avoiding water absorption. The surfaces were characterized with SEM, EDS, XRD techniques, roughness, sessile water drop contact angle, surface energy measurements, and standard antimicrobial tests. The surface hydrophobicity and the antimicrobial activity results were compared with that of unmodified, uncoated gloss fired wall tiles. A superhydrophobic contact angle of 150° was achieved at 1000 °C peak temperature due to the formation of micro-structured nanocrystalline zinc oxide granules providing a specific surface topography. At higher peak temperatures the hydrophobicity was lost as the specific granular surface topography deteriorated with the conversion of zinc oxide granules to the ubiquitous willemite crystals embedded in the glassy matrix. The antimicrobial efficacy also correlated with the hydrophobic character.

1. Introduction

Hydrophobic surfaces are defined as having sessile water drop contact angle greater than 90°, while surfaces with contact angles larger than 150° are rendered as superhydrophobic. The surface chemistry and morphology are the major factors determining hydrophobicity [1–6]. The Young's model states that a smooth solid surface with a lower free energy has a higher sessile liquid drop contact angle since any isolated system changes to achieve a minimum free energy. Whether a smooth surface is hydrophilic or hydrophobic depends on the solid-liquid and solid-air interfacial energies [7]. In order to explain the phenomena related to rough surfaces Wenzel [8] and Cassie-Baxter [9] basic models are employed. Wenzel model states that the contact between a rough solid surface and a liquid is uninterrupted, and the increased surface area of the solid due to roughness causes a chemically hydrophilic surface to have a further decreased contact angle, while on a chemically hydrophobic surface the contact angle rises above that of the smooth surface. However, Cassie-Baxter model assumes air pockets to be trapped between the rough solid surface and the liquid, and a chemically hydrophilic surface may become hydrophobic and vice versa depending on the solid-air, liquid-air interfacial energies. The superhydrophobicity is a required property especially for keeping the surfaces free of wetting, and thus avoiding contamination by water based slurries, suspensions, and solutions. These types of surfaces are also classified as self-cleaning due to the difference in advancing and receding contact angles [10–14].

Hydrophobic surfaces are also known to have non-migrating antimicrobial character by restricting the adherence of microorganisms on the surface [15]. Since the inhibiting effect is not due to the consumption of any antimicrobial agent, and is only physical, advantageously any immunity development is not possible [16,17]. Nevertheless, antibacterial ceramic tile surfaces with a biocidal antimicrobial molecular barrier coating were developed as an alternative to hydrophobic surfaces [18]. Antimicrobial floor and wall coating materials in clinical, industrial and household spaces,

* Corresponding author.
E-mail address: selcuk.ozcan@bilecik.edu.tr (S. Özcan).

https://doi.org/10.1016/j.apsusc.2017.08.014
0169-4332/

Table 1
Sessile water drop/ceramic surface contact angles, and ceramic surface free energies.

Tile surface type/Heat treatment peak temperature and duration	Industrial glaze contact angle	Industrial glaze + polymer coating contact angle	Zn modified glaze contact angle	Zn modified glaze + polymer coating contact angle	Zn modified glaze + polymer coating overall SFE (γ_{sg})
980 °C, 5 min	~40°	~70°	125° → absorbed	125°–135°	11.3 mJ/m^2
1000 °C, 5 min	<30°	~70°	130° → absorbed	145°–150°	5.40 mJ/m^2
1050 °C, 5 min	<30°	~70°	55° → absorbed	115°–120°	16.0 mJ/m^2
1100 °C, 5 min	<30°	~70°	50° → absorbed	90°–95°	29.7 mJ/m^2
1050 °C, 60 min	<30°	~70°	50° → absorbed	85°–90°	34.2 mJ/m^2
1100 °C, 30 min	<30°	~70°	50° → absorbed	80°–85°	41.3 mJ/m^2

Table 2
Surface roughness parameters.

Tile surface type/Heat treatment peak temperature and duration	Industrial glaze surface roughness		Zn modified glaze surface roughness	
	Ra (μm)	Rz (μm)	Ra (μm)	Rz (μm)
980 °C, 5 min	–	–	450	2200
1000 °C, 5 min	2.6	18	540	2900
1050 °C, 5 min	–	–	370	2000
1100 °C, 5 min	–	–	70	300
1050 °C, 60 min	–	–	60	270
1100 °C, 30 min	–	–	40	220

especially on wettable surfaces is demanding, with a potential to reduce the hospital infections and various dermatome risks [19].

Ceramic coating products are produced by heat treatment for sintering and vitrification, and the vitrified matrix of the surface is inevitably hydrophilic due its water attracting chemistry [20]. Imparting a hydrophobic character on a gloss fired ceramic surface depends on the formation of nano or micro patterned surface topography by the nano or micro sized granular structures on the glazed or full body ceramic tile surfaces. In nature there are a number of examples of superhydrophobic plant or animal shell surfaces due to surface topography rather than surface chemistry such as the lotus flower leaves and the snail shell [21,22].

The wettability of diverse liquids of many different surfaces was also studied extensively [23,24] and superhydrophobic surfaces including alumina ceramics, silica hybrid films, and titania coatings on float glass were constructed by a number of methods such as thermal spray, laser texturing, vapor-fed aerosol flame synthesis, and sol-gel route methods [25–27]. None of these methods have the potential of application in the conventional ceramic wall tile production lines.

Zinc oxide nanoparticles are known to exhibit antibacterial activity that depends on the localized interaction of ZnO in terms of increased membrane permeability, direct endocytosis of nanoparticles, and the uptake of dissolved zinc ions, interfering with the intracellular metabolism. The effect of ZnO particle size, concentration, morphology, porosity, defects, and particle surface modifications on the bacterial and fungal inhibition were extensively studied [28–31]. The applications can be topical or systemic, however, the inconvenience of the diffusion and consumption of the migrating bactericidal component for ceramic coating materials necessitates to develop hydrophobic and hence non-migrating bactericidal or bacteriostatic ceramic tile surfaces.

In this study, body fired ceramic wall tiles were coated with industrially applicable glazes modified with the inclusion of metallic zinc powder, which is suitable for gloss firing in the already existing conventional wall tile production lines. The effects of the formation of micro-structured zinc oxide (ZnO), and willemite ($2ZnO.SiO_2$) crystals on the gloss fired tile surface topography and/or chemistry as the peak gloss firing temperature and duration was changed, which in turn affecting the hydrophobicity and antibacterial character, were determined.

2. Materials and methods

2.1. Ceramic tile coating and sintering

The green ceramic wall tile bodies were fired in an industrial ceramic furnace (roller, open hearth) of 90 m long for a firing cycle of 28 min with the firing zone maximum temperature of 1140 °C. The body fired wall tiles were coated with a modified glaze by pressurized air spraying. The glaze was modified with the addition of metallic zinc powder into an industrially applicable glaze composition prior to aqueous milling. The glaze composition was prepared as 30% frit (boric acid 15%, alumina 3%, quartz 27%, potassium feldspar 35%, potassium nitrate 2%, calcite 15%, magnezite 3%, 3 ppt sodium carboxymethyl cellulose, 1.5 ppt sodium tripolyphosphate), 5% china clay, and 65% metallic Zn powder, all percentages being by weight for the rest of the document. The metallic zinc powder was obtained from the manufacturer Hepsen Kimya Ltd., Bilecik, Turkey, under the brand name of "Zinc Powder Blue" with the technical specifications as follows. The particles under 32 μm was 99.1%, total zinc content was 97%, metallic zinc content was 94%, Pb content was 0.03%, and Fe content was 0.15%. The modified glaze was prepared in ceramic jar jet mills rotated at 120 rpm for 20 min with a milling load of alumina balls and in water medium with 35% water and 65% dry matter. The glaze slurry was sieved through 45 μm. The coated tiles were fired in a laboratory muffle kiln at the maximum temperatures of 980 °C (5 min), 1000 °C (5 min), 1050 °C (5 min, and 60 min), 1100 °C (5 min, and 30 min) with a heating rate of 30 °C/min below 500 °C and 5 °C/min above 500 °C. Some of the sintered tiles were further processed by spray coating with a commercial polymeric composition of 10% fluoropolymer, 60% alkoxysilane and 30% ethanol, under the trade name ECC-4000, and curing at 120 °C for 10 min in order to avoid water absorption and to enhance the hydrophobic character. The sprayed quantity was approximately 250 g/m^2.

2.2. Tile surface characterization

The contact angle and surface free energy (SFE) measurements were carried out by drop shape analyzer (Kruss, DSA-25), using water and diiodomethane as liquids of known surface tensions (ST) in air. The SFE calculations were done according to Young's equation (Eq. (1)) and a two-component model developed by Fowkes [32],

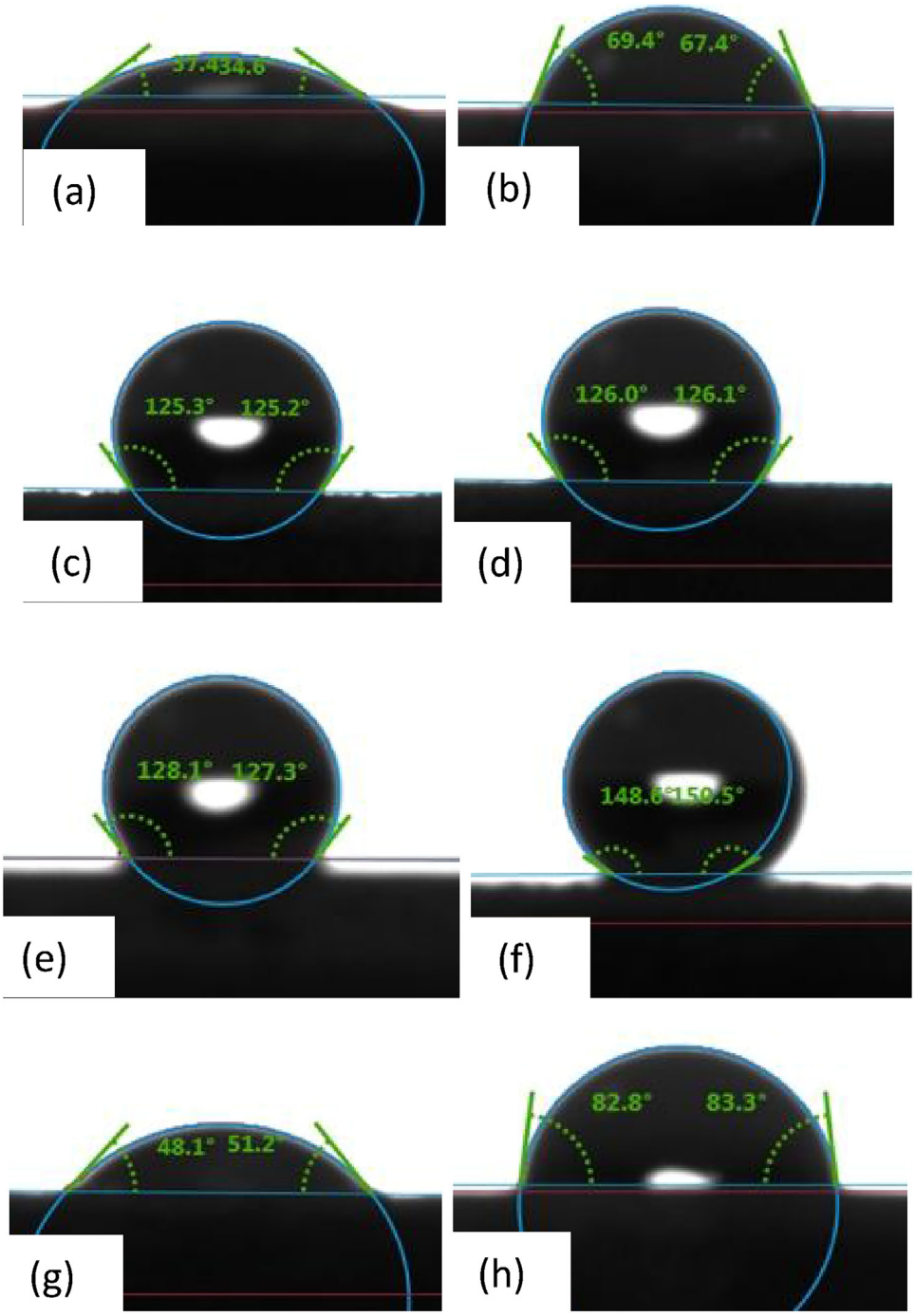

Fig. 1. Sessile water drop contact angles with the ceramic tile surfaces of (a) unmodified, uncoated, (b) unmodified, polymer coated, (c) Zn modified fired at 980 °C peak temperature for 5 min, and uncoated, (d) Zn modified fired at 980 °C peak temperature for 5 min, and polymer coated, (e) Zn modified fired at 1000 °C peak temperature for 5 min, and uncoated, (f) Zn modified fired at 1000 °C peak temperature for 5 min, and polymer coated, (g) Zn modified fired at 1100 °C peak temperature for 30 min, and uncoated, (h) Zn modified fired at 1100 °C peak temperature for 30 min, and polymer coated.

and Owens, Wendt, Rabel and Kaelble (OWRK method) [33,34]. In the two-component model [35] it is assumed that ST of the liquids and SFE of the solid have disperse and polar components as additive parts (Eqs. (2) and (3)), and the interfacial tension (IFT) between a liquid and the solid is given by the so called geometric mean method (Eq. (4)).

$$\gamma_{sl} = \gamma_{sg} - \gamma_{lg} \cos\ \theta \tag{1}$$

$$\gamma_{lg} = \gamma_{lg}^{D} + \gamma_{lg}^{P} \tag{2}$$

$$\gamma_{sg} = \gamma_{sg}^{D} + \gamma_{sg}^{P} \tag{3}$$

$$\gamma_{sl} = \gamma_{sg} + \gamma_{lg} - 2\left(\sqrt{\gamma_{lg}^{D}\gamma_{sg}^{D}} + \sqrt{\gamma_{lg}^{P}\gamma_{sg}^{P}}\right) \tag{4}$$

where, θ is the contact angle between the solid and the sessile liquid drop, γ_{lg}, γ_{lg}^{D} and γ_{lg}^{P} are the overall, disperse and polar components of the ST of the liquid, γ_{sg}, γ_{sg}^{D} and γ_{sg}^{P} are the overall, disperse and polar components of the SFE of the solid, respectively. Eqs. (1) and (4) are combined yielding Eq. (5) that allows the calculation of the disperse and polar components of the SFE of the solid by measuring

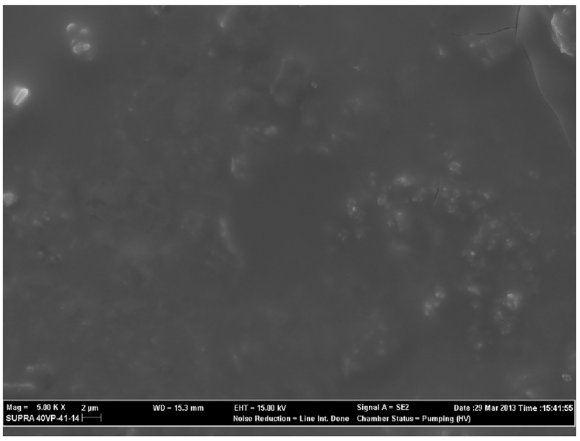

Fig. 2. SEM image of the ceramic wall tile with unmodified glaze gloss fired at 1000 °C peak temperature for 5 min.

the contact angle of sessile drops of two different liquids of known disperse and polar ST components.

$$\gamma_{lg}\left(1+\cos\ \theta\right)=2\left(\sqrt{\gamma_{lg}^{D}\gamma_{sg}^{D}}+\sqrt{\gamma_{lg}^{P}\gamma_{sg}^{P}}\right) \tag{5}$$

Eq. (5) can be simply solved for γ_{sg}^{D} and γ_{sg}^{P} (Eqs. (6), (7)) when one of the liquids is chosen to have only either disperse or polar ST component, as in the case of diiodomethane (liquid 1), the polar ST component of which equals zero. The other liquid can have both disperse and polar ST components as water (liquid 2) [36–38].

$$\gamma_{sg}^{D}=\frac{\gamma_{l1g}^{2}\left(1+\cos\ \theta_1\right)^{2}}{4\gamma_{l1g}^{D}},\ \text{and since}\ \gamma_{l1g}=\gamma_{l1g}^{D},$$

$$\gamma_{sg}^{D}=\frac{1}{4}\gamma_{l1g}\left(1+\cos\ \theta_1\right) \tag{6}$$

$$\gamma_{sg}^{P}=\frac{1}{\gamma_{l2g}^{P}}\left(\frac{1}{2}\gamma_{l2g}\left(1+\cos\ \theta_2\right)-\sqrt{\gamma_{l2g}^{D}\gamma_{sg}^{D}}\right)^{2} \tag{7}$$

At the measurement temperature of 20 °C, $\gamma_{l1g}=\gamma_{l1g}^{D}=50.8\ mN/m$, $\gamma_{l1g}^{P}=0\ mN/m$ (values for diiodomethane), and $\gamma_{l2g}=72.8\ mN/m$, $\gamma_{l2g}^{P}=46.4\ mN/m$, $\gamma_{l2g}^{D}=26.4\ mN/m$ (values for water) [35,39,40].

The surface roughnesses of the ceramic surfaces were determined with Mitutoyo SJ-301 surface roughness tester in the roughness profile mode, and the curves were corrected by Gaussian filter in accord with JIS B0601-2001. Arithmetic mean deviation of the troughs and crests from the mean line of the roughness profile (Ra), and maximum trough to crest height mean of irregularities of ten-sampling lenghts (Rz) were recorded as roughness parameters.

The phases and microstructure of the tile surfaces were characterized by XRD at 2θ between 10°–80° with a scan rate of 3.5°/min (Pananalytical Empyrean, Cu-Kα radiation), and SEM-EDX (FEI, NOVANANOSEM 650 with field emission gun, high voltage 2.00–20.0 kV, work distance 5.0–6.3 mm, and Zeiss, Supra 40 VP, with high voltage 10.0 kV, work distance 10.2–13.2 mm), respectively.

The antimicrobial tests were carried out in accordance with ASTM E2180-07 (Standard test method for Determining the Activity of Incorporated Antimicrobial Agent in Polymeric or Hydrophobic Materials) with the bacteria *Staphylococcus aureus* ATCC 6538 and *Pseudomonas aeruginosa* ATCC 15442 at Egemikal Lab, Ege University, Izmir, Turkey.

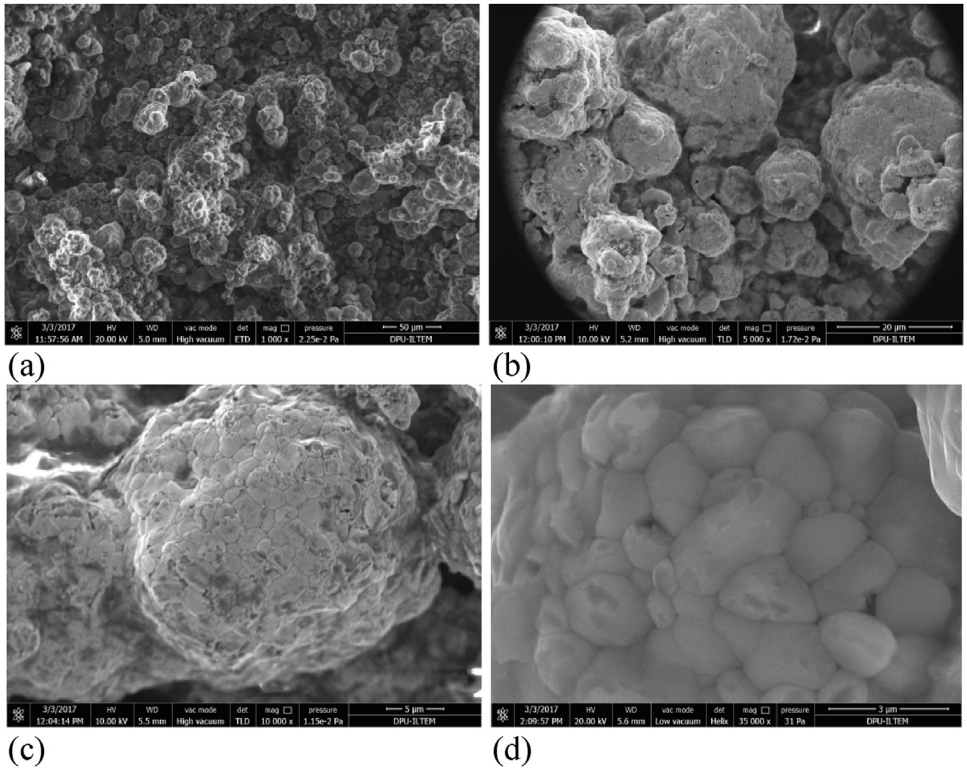

Fig. 3. SEM image of the tile surface with the zinc modified glaze and gloss fired at 980 °C for 5 min at various magnifications.

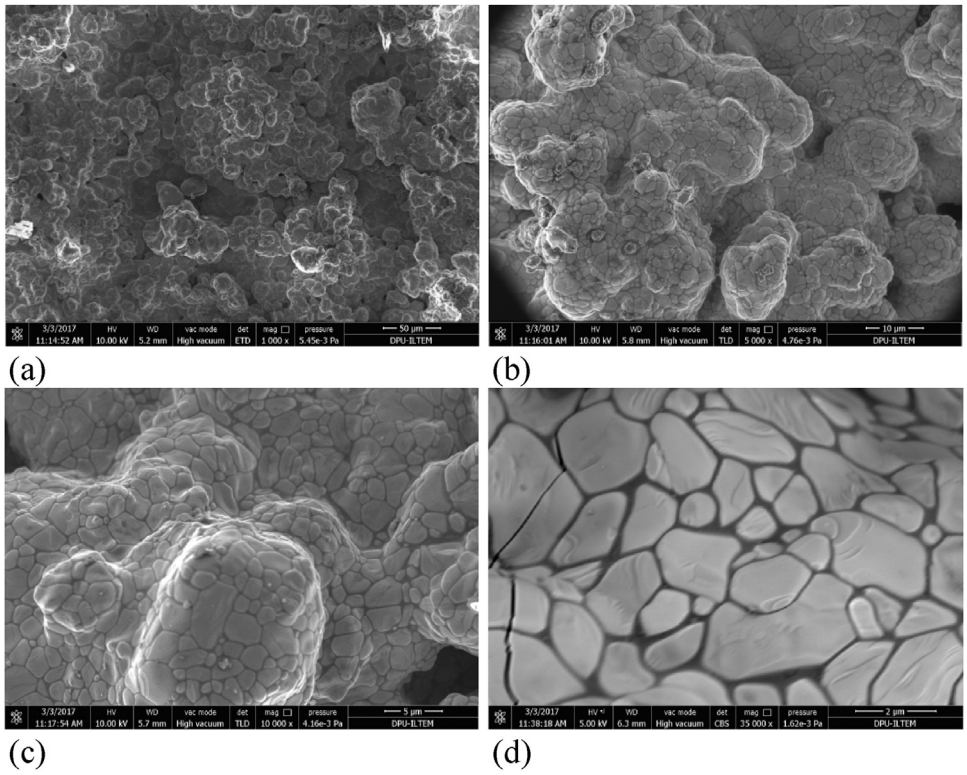

Fig. 4. SEM image of the tile surface with the zinc modified glaze and gloss fired at 1000 °C for 5 min at various magnifications.

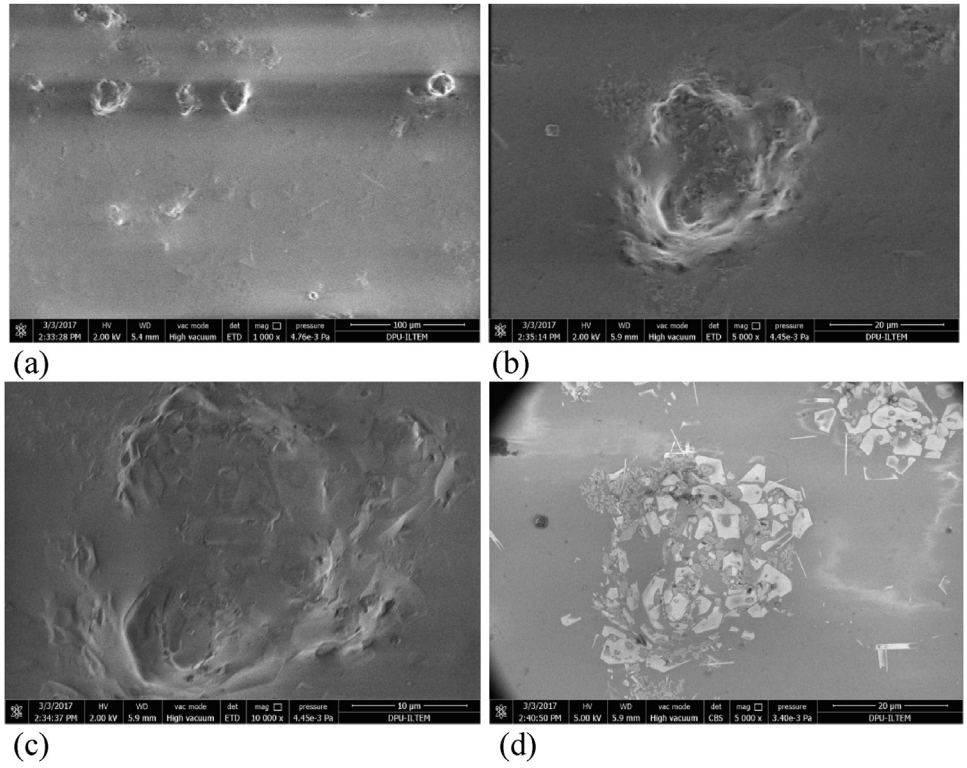

Fig. 5. SEM image of the tile surface with the zinc modified glaze and gloss fired at 1050 °C for 5 min at various magnifications.

3. Results and discussion

In order to exploit the plausibility of developing hydrophobic and antimicrobial ceramic tile surfaces, the wall tile glaze composition of a local tile manufacturer was modified with the addition of Zn metal powder in the glaze as 65% of the total dry matter, and gloss fired. The increasing intensity of the heat treatment in terms of the peak temperature as the major and duration as the minor

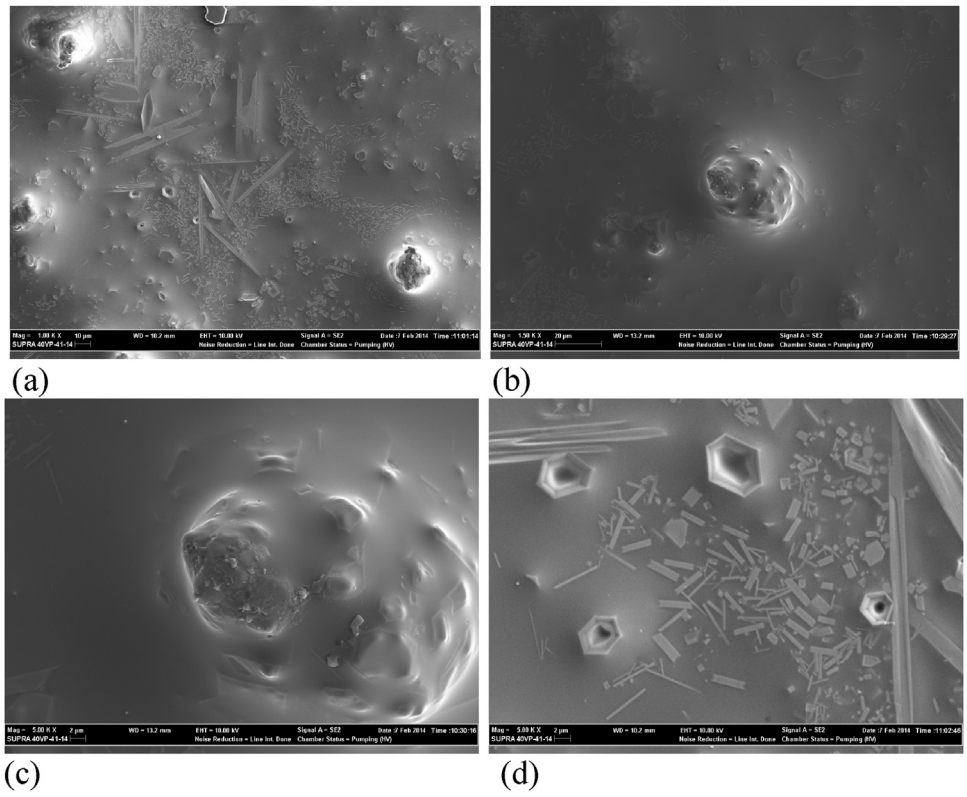

Fig. 6. SEM image of the tile surface with the zinc modified glaze and gloss fired at 1100 °C for 5 min at various magnifications.

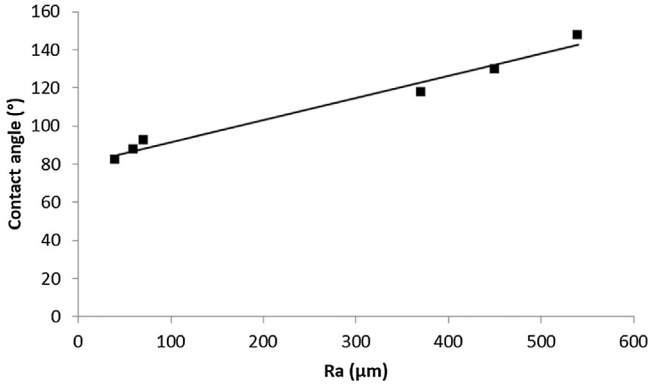

Fig. 7. Sessile water drop contact angle of the Zn modified, gloss fired and polymer coated ceramic tile surface versus surface roughness parameter Ra of the underlying surface (uncoated corresponding surface).

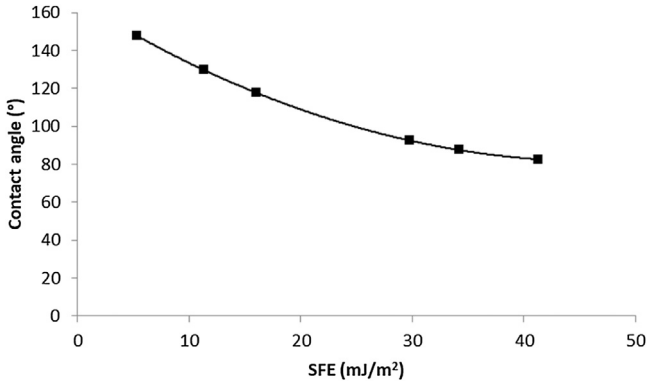

Fig. 8. Sessile water drop contact angle versus the surface free energy of the Zn modified, gloss fired and polymer coated ceramic tile surface.

factors was correlated with the sessile water drop contact angle, and the surface free energy of the surface. The results are summarized in Table 1. The surface roughness parameters Ra and Rz were provided in Table 2 (Ra and Rz values were given to two significant figures accuracy).

The contact angles of the sessile water drops with various tile surfaces heat treated at different heat intensities are shown in Fig. 1. All of the contact angles of the gloss fired tile surfaces with the industrial glaze (unmodified) at all heat treatment temperatures were low, below 30°, with the exception at 980 °C which was 40°. The polymer coating on these gloss fired tiles provided a contact angle of 70° regardless of the heat treatment temperature. The increase in the contact angle from 30° to 70° indicated the change of the surface chemistry to a less hydrophilic state. The SEM image of the ceramic wall tile with the unmodified glaze gloss fired at 1000 °C peak temperature for 5 min is shown in Fig. 2. The surface was almost smooth and featureless as supported by its surface roughness (Ra = 2.6 μm) in comparison to the tiles with the modified glaze (40 μm < Ra < 540 μm).

However, the gloss fired tiles with the zinc modified glaze but without the polymeric coating, even though the initial contact angles were large, completely absorbed the water droplet, the contact angle dropping to zero in a few minutes. This phenomenon was due to the fact that the zinc modified glaze did not vitrify enough to provide a glassy surface at none of the heat treatment temperatures. The sintered granular surface structure was porous absorbing water, as revealed by the SEM images given in Figs. 3–6. The highest initial contact angle reached was 130° for the tiles fired at the peak temperature of 1000 °C. For the heat treatments above that temperature the initial contact angles dropped abruptly. When these surfaces were covered with the non-porous polymer layer, the water absorption was avoided and the contact angles at all the heat treatment temperatures were increased as compared to their

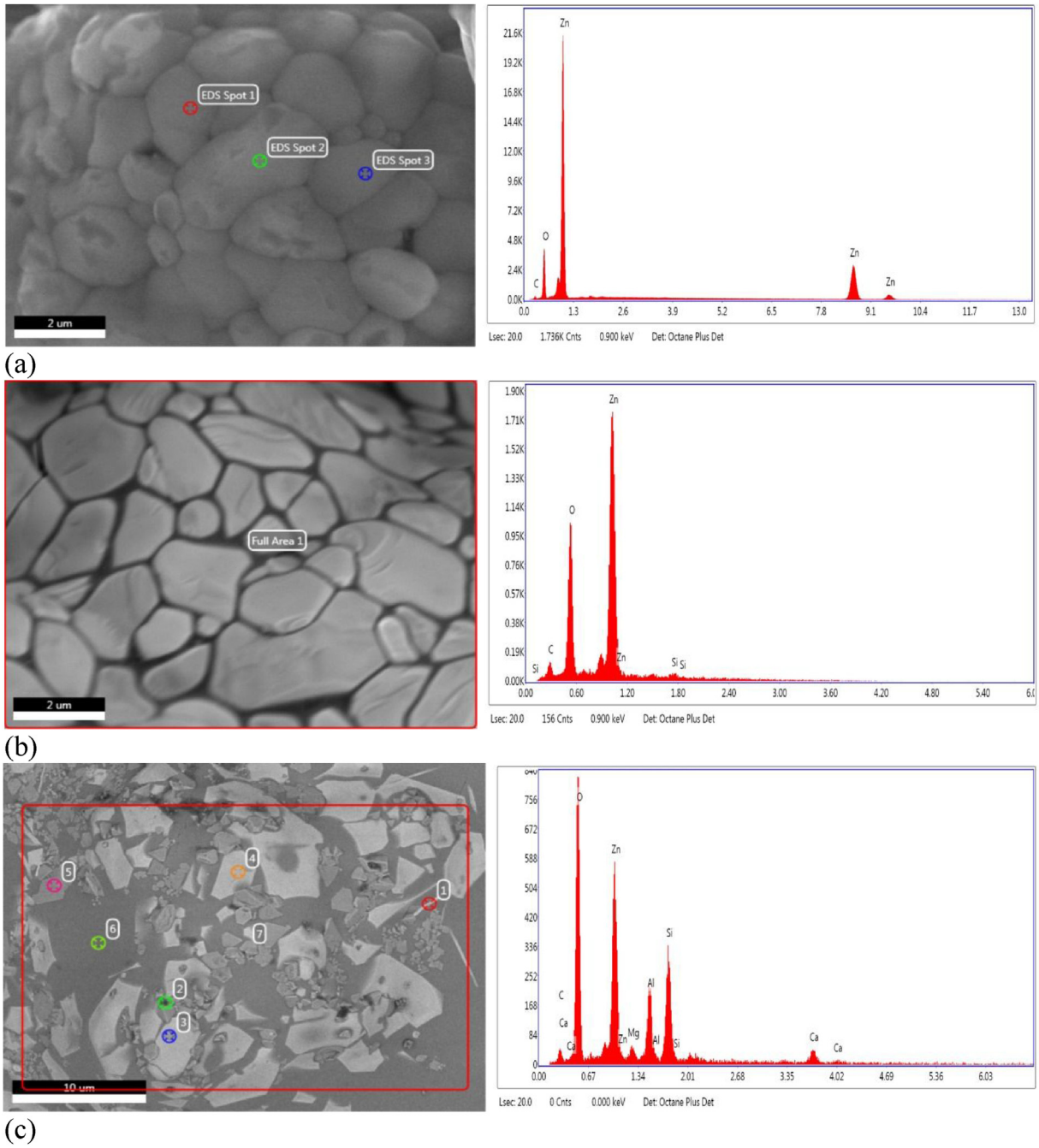

Fig. 9. EDX analysis of tile surface with the zinc modified glaze, (a) gloss fired at 980 °C for 5 min, (b) gloss fired at 1000 °C for 5 min, (c) gloss fired at 1050 °C for 5 min.

uncoated counters. Again the highest contact angle of 150°, promisingly on the superhydrophobic limit, was reached for the tiles gloss fired at the peak temperature of 1000 °C. For heat treatments above 1050 °C the achieved contact angles decreased to the hydrophilic range of 90°–80°.

The SEM images in Figs. 3 and 4 indicated that the high contact angles obtained at the peak temperatures of 980 °C and 1000 °C were attributable to the microscale surface topography generated by the incorporation of the Zn metal powder in the glaze. The microscale surface pattern formed was reminiscent of the naturally ultrahydrophobic lotus flower leaf [21]. The contact angle decreased for the surfaces heat treated at the peak temperatures above 1000 °C. The granular micro-pattern was deteriorated rapidly starting at 1050 °C and ubiquitous crystals formed in the glaze as shown in Figs. 5 and 6. The increase of the sessile water drop contact angle of the modified glaze, gloss fired and polymer coated tile surfaces with the increasing surface roughness of the respective uncoated surfaces, Ra, as shown in Fig. 7, confirmed that the specific surface topography was effective in achieving high contact angles in the hydrophobic range.

The surface free energies of the Zn modified, gloss fired and polymer coated ceramic tile surfaces were well correlated with the contact angles as depicted in the contact angle versus surface free energy graph given in Fig. 8. The quantitative data obtained for the specific surfaces under examination suggested that a lower surface energy imparted a higher contact angle, and the slope of the curve leveled off gradually with increasing surface energy. Thus as empirically shown, lowering the surface free energy was essential

in achieving a superhydrophobic surface in accord with theoretical considerations.

The ceramic wall tiles with the unmodified glaze gloss fired above 1000 °C had smooth hydrophilic surfaces with contact angles less than 30°. When the surface was covered with the polymer, the surfaces remained hydrophilic with contact angles of approximately 70°. A smooth surface is hydrophilic when $\gamma_{sl} < \gamma_{sg}$ and hydrophobic when $\gamma_{sl} > \gamma_{sg}$ according to Young's model. The tiles with Zn metal modified glazes gloss fired at peak temperatures 980 °C–1050 °C for 5 min duration had rough hydrophobic surfaces with water contact angles between 115°–150°. According to Cassie-Baxter model this is possible when air pockets is entrapped between liquid drop and rough surface, and a chemically hydrophilic surface can become hydrophobic or superhydrophobic due to surface morphology when $\gamma_{lg} > \gamma_{sg}$.

The EDX analyses results given in Fig. 9 showed that the metallic zinc powder added into the commercial glaze was oxidized yield-

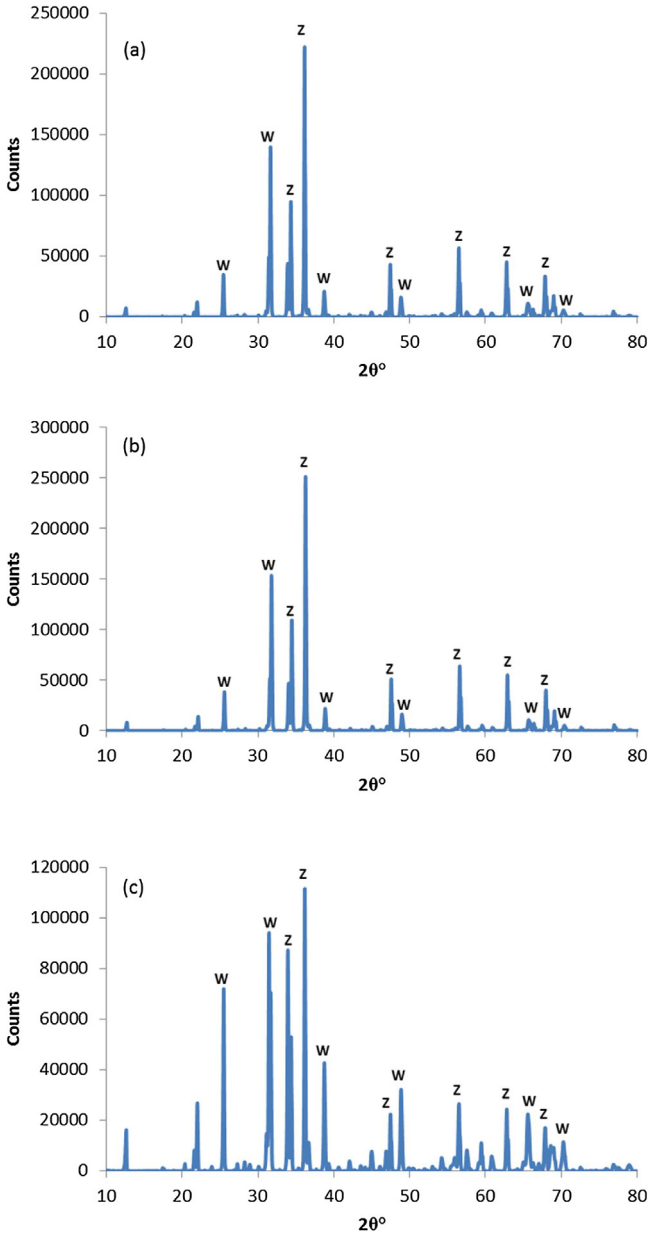

Fig. 10. XRD patterns of the ceramic tile surfaces gloss fired at the peak temperature of (a) 980 °C for 5 min, (b) 1000 °C for 5 min, (c)1050 °C for 5 min, (d) 1100 °C for 5 min, (e) 1050 °C for 60 min, (f) 1100 °C for 30 min.

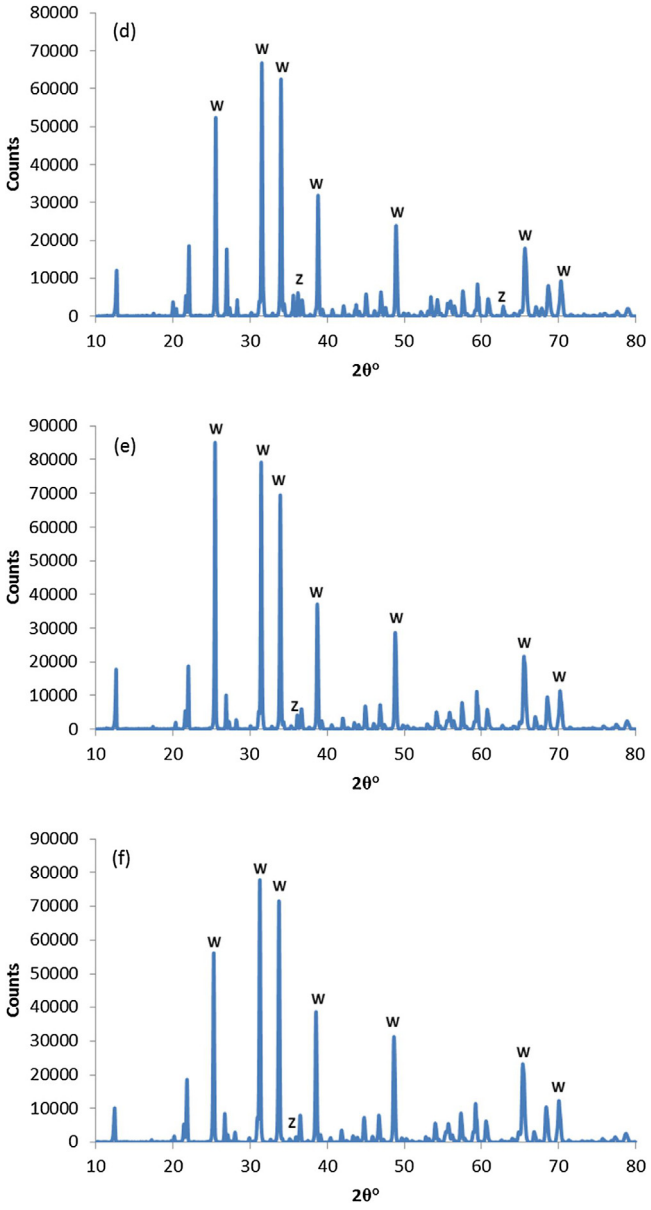

Fig. 10. (*Continued*)

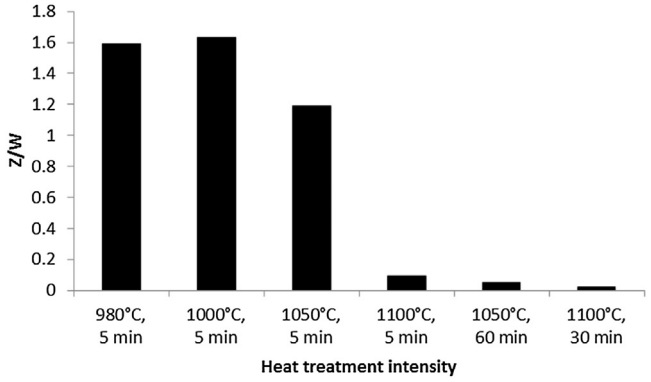

Fig. 11. Largest zinc oxide (ZnO) and willemite ($2ZnO.SiO_2$) XRD peak height ratios (Z/W) versus heat treatment intensity.

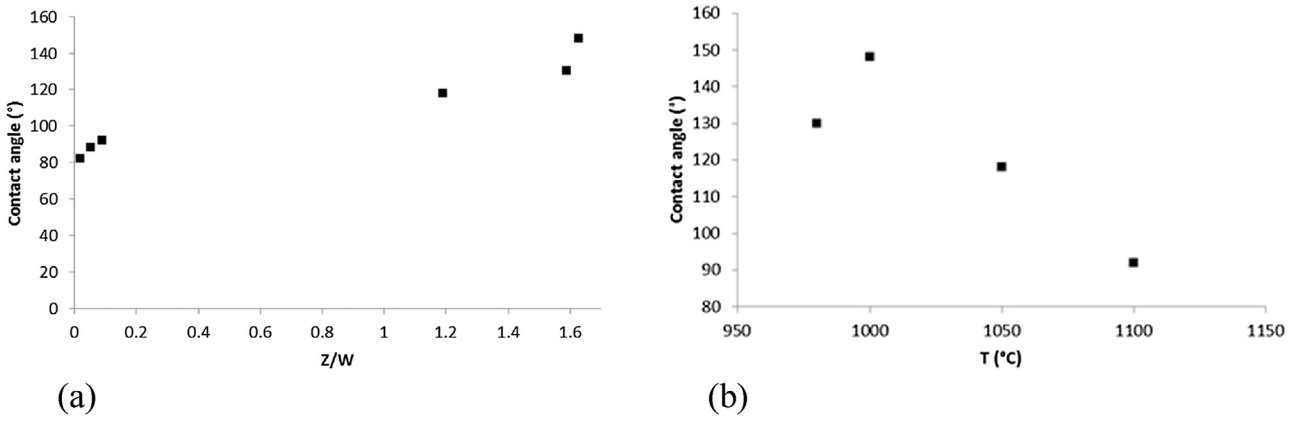

Fig. 12. (a) Sessile water drop contact angle of the Zn modified, gloss fired and polymer coated ceramic tile surface versus (a) zinc oxide/willemite crystal XRD peak height ratio (Z/W), (b) heat treatment peak temperature.

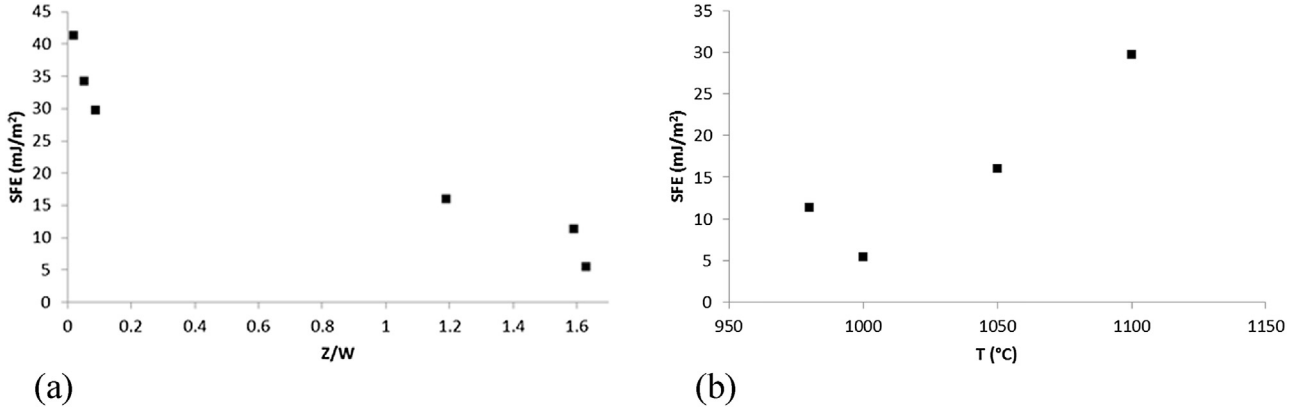

Fig. 13. Surface free energy (SFE) of the Zn modified, gloss fired and polymer coated ceramic tile surface versus (a) zinc oxide/willemite crystal XRD peak height ratio (Z/W), (b) peak heat treatment temperature.

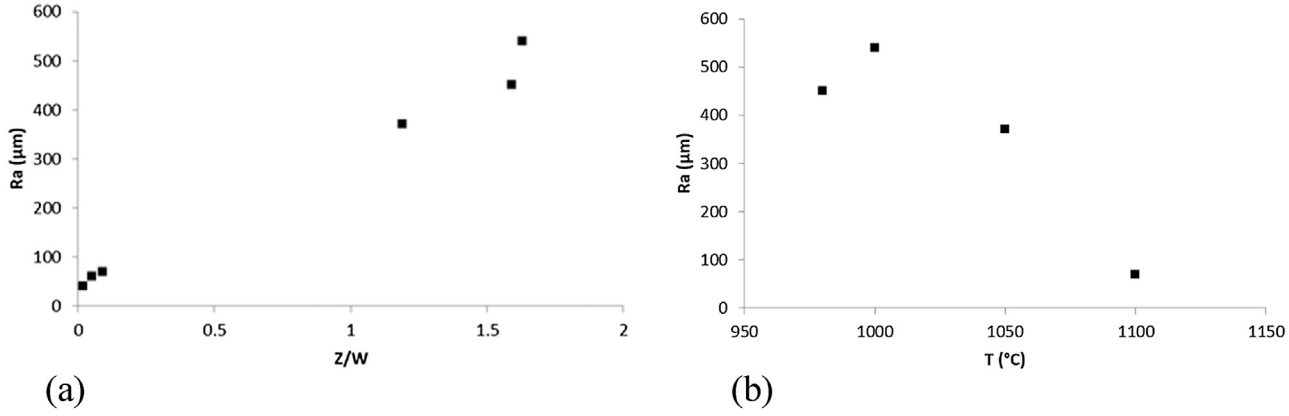

Fig. 14. Surface roughness (Ra) of the Zn modified, gloss fired, uncoated ceramic tile surface versus (a) zinc oxide/willemite crystal XRD peak height ratio (Z/W), (b) peak heat treatment temperature.

ing mainly ZnO crystals. Nevertheless, for the tiles sintered at 980 °C (Fig. 9a) the oxidation of the metallic zinc was partial as evidenced by the high ratio of Zn/O atomic percentages. The atomic % of zinc was in the range 58%–67%, while for oxygen it was 24%–31%. Therefore, Zn/O ratio was in between 1.9 to 2.8. For the heat treatment at the peak temperature of 1000 °C (Fig. 9b) the atomic percent of zinc was in the range 32%–38% and oxygen was in the range 48%–51% making the Zn/O ratio 0.65–0.77 which indicated a complete oxidation of the metallic zinc and the existence of other oxides in little amounts. When the heat treatment peak temperature was raised to 1050 °C (Fig. 9c) the atomic percentages of the elemental species on the average were oxygen 56%, zinc 11%, silicon 14%, aluminum 7.2%, calcium 2.6%, and magnesium 1.2%. This indicated that most probably the crystalline oxide forms, ZnO, SiO_2, Al_2O_3, and a glassy matrix of mainly CaO, MgO, SiO_2, ZnO were prominent.

The XRD analyses given in Fig. 10 provided definitive evidence of the formation of majorly zinc oxide (ZnO) and willemite ($2ZnO.SiO_2$) crystals at all of the heat treatment temperatures. The ratios of the largest peak heights of the ZnO crystals (at $2\theta = 36.1^\circ$) to $2ZnO.SiO_2$ crystals (at $2\theta = 31.5^\circ$) in the XRD patterns, abbreviated

Table 3
Microbial tests of the industrial, polymer coated industrial, and polymer coated Zn modified glazed tiles.

Microorganism	Tile Sample	Count in the control sample (cfu/mL[a])	Count after surface application (cfu/mL)	Percent decrease	Change with respect to industrial tile surface
Staphylococcus aureus (ATCC 6538)	Industrial tile	210,000	6000	97.1%	0
	Polymer coated industrial tile	210,000	93,000	55.7%	+15.5 folds
	Polymer coated Zn modified glazed tile	210,000	19	99.991%	−99.7%
Pseudomonas aeruginosa (ATCC 15442)	Industrial tile	560,000	30,000	94.6%	0
	Polymer coated industrial tile	560,000	35,000	93.8%	+1.17 folds
	Polymer coated Zn modified glazed tile	560,000	4000	99.3%	−86.7%

[a] cfu/mL: colony forming unit per milliliter.

as Z/W, were determined as a function of heat treatment intensity as depicted in Fig. 11. The Z/W ratio passed through a maximum with the increasing heat treatment intensity. The maximum value of Z/W was 1.63 at the peak temperature of 1000 °C for 5 min duration, above which it decreased, and the decrease was abrupt over 1050 °C. The minimum value was determined as 0.019 indicating that the ZnO granules were essentially converted to willemite crystals. The SEM and EDS images (Fig. 9) confirmed the conversion as the almost total loss of the granular surface topography, and with the indicative elemental compositions.

The correlations between the sessile water drop surface contact angle and the Z/W ratio, and between the sessile water drop surface contact angle and the heat treatment peak temperature are shown in Fig. 12a and b. The contact angle increased with the Z/W, and passed through a maximum with increasing heat treatment peak temperature at 1000 °C for which also the Z/W was maximum. The correlations between the surface free energy and the Z/W ratio, or the heat treatment peak temperature existed as the reverse trends as seen in Fig. 13a and b. This phenomenon was most probably due to the changing surface topography as confirmed by decreasing surface roughness with the decreasing Z/W. The roughness reached its maximum at 1000 °C peak temperature as in the case of the contact angle as shown in Fig. 14a and b. The ZnO crystalline granules were rapidly formed in the particular structure and distribution by the oxidation of the metallic zinc powder bringing about the hydrophobic surface topography up to 1000 °C. By the increasing peak heat treatment temperature the granular zinc oxide crystals were converted to the willemite crystals by partially melting and diffusing into the surrounding glassy matrix and reacting with SiO_2, which in turn became embedded in the glassy matrix. Above 1050 °C the surface topography was almost completely destroyed, smoothing out the surface as indicated by the SEM images and the surface roughness measurements. If ZnO was directly used instead of metallic zinc the conversion to willemite and the deterioration of the specific surface topology would take place at lower temperatures well before any glaze vitrification. The change of the contact angle with the peak heat treatment temperature also indicated that the hydrophobicity of the surface reached a maximum at 1000 °C and became hydrophilic above 1050 °C, in accordance with the crystalline structural change of the surface.

Although the polymer coating changed the surface chemistry completely it had only a slight contribution to the hydrophobicity apart from hindering water absorption. Therefore, it was concluded that the induced hydrophobicity was due to the particular surface topography generated by the crystalline zinc oxide granules rather than the chemical structure of the surface. The thickness of the polymer layer was estimated by calculation to be approximately 150 μm on the average, corresponding to the 250 g/m^2 spray application, 70% polymer yield and 1.2 g/cm^3 polymer density. The thickness of the polymer layer on the crests was expected to be less than the average, while it was more on the troughs preserving or even bringing about a more prominent surface structure for a hydrophobic topography in conformity with the Cassie-Baxter model.

The antimicrobial tests were conducted on the tile surfaces with the unmodified, and the Zn modified glazes, and gloss fired at the peak tempearture of 1000 °C for 5 min, coated with the polymer. The industrial tile (unmodified) gloss fired at 1000 °C for 5 min which was not coated with the polymer was used as the reference sample. The results are given in Table 3. The antimicrobial tests indicated that the bacterial activity (quantified as colony forming unit per milliliter, cfu/mL) with the bacterium *Staphylococcus aureus* on the unmodified but the polymer coated surface increased 15.5 folds while on the Zn modified and polymer coated surface decreased by 99.68%, and with the bacterium *Pseudomonas aeruginosa* on the unmodified but polymer coated surface increased 1.17 folds while on the Zn modified and polymer coated surface decreased by 86.7%, as compared to the unmodified, uncoated surface. The drastic decrease in the antimicrobial activity of the ceramic tile surfaces with the crystalline ZnO granules was correlated directly to the increased surface hydrophobicity. The drastic increase in the bacterial activity on the polymer coated unmodified surfaces pointed to a convenient surface chemistry for the bacterial proliferation. However, the induced hydrophobicity totally cancelled out this adverse condition, indicating that the surface hydrophobicity was by far the major determining factor for the deterrence of microbial growth and proliferation.

4. Conclusions

Inclusion of metallic zinc powder in an industrially applicable glaze resulted in the formation of nanocrystalline ZnO granules up to the peak heat treatment temperature of 1000 °C for 5 min duration providing a micro-patterned surface topography. The granular surface topography started to deteriorate above 1000 °C, and almost completely destroyed over 1050 °C. At these elevated temperatures the zinc oxide (ZnO) crystals partially melted and diffused in to the glassy matrix and reacted with quartz (SiO_2) producing the ubiquitous willemite ($2ZnO.SiO_2$) crystals. The change of the sessile water drop contact angle with the peak heat treatment temperature indicated that the hydrophobicity of the surface reached a maximum at 1000 °C with a contact angle of 150° of the superhydrophobic limit, and became hydrophilic above 1050 °C, in accordance with the crystalline structural change of the surface. This specifically evidenced the existence of a correlation between the sessile drop surface contact angle and the $ZnO/2ZnO.SiO_2$ ratio. The polymer coating on the ceramic tile surfaces functioned only as a water impermeable layer, and the induced hydrophobicity was due to the particular surface topography generated by the nanocrystalline zinc oxide granules rather than the chemical structure of the surface.

The micro-patterned surface topography of the nanocrystalline ZnO granules also imparted an antimicrobial character to the ceramic tile surfaces which was well correlated with the hydrophobicity. The bacterial proliferation on the tiles with the zinc modified glaze was suppressed up to over 99%.

The study paves the way to the development of commercial hydrophobic and antimicrobial ceramic wall tiles. Although the polymer layer covalently bonds to the underlying structure and was reported to withstand for over two years, the alternative approach may be the use of zinc metal modified glazes as an engobe layer covered with a few hundred micrometer thick, low temperature melting glaze.

Acknowledgements

This work was financially supported by Bilecik Şeyh Edebali University, Scientific Research Fund [project number 2012-01-BIL.03-03]; and UNESCO-Loreal project support to N. Calis Acikbas (2014-2015).

References

[1] A. Nakajima, K. Hashimoto, T. Watanabe, Recent studies on superhidrophobic films, Monatschefte für Chemia 132 (2001) 31–41.
[2] A. Torkeli, Droplet Microfluidics on a Planar Surface, Dissertation for the Degree of Doctor of Science in Technology, Helsinki University, Espoo, 2003.
[3] W. Chen, Y.A. Fadeev, C.M. Hsieh, D. Oner, J. Youngblood, T. McCarthy, Ultrahydrophobic and ultralyophobic surfaces: some comments and examples, Langmuir 15 (1999) 3395–3399.
[4] D. Oner, T. McCarthy, Ultrahydrophobic surfaces: effects of topography length scales on wettability, Langmuir 16 (2000) 7777–7782.
[5] M. Miwa, A. Nakajima, A. Fujisima, K. Hashimoto, T. Watanabe, Effects of the surface roughness on sliding angles of water droplets on superhydrophobic surfaces, Langmuir 16 (2000) 5754–5760.
[6] E.R. Johnson, H.R. Dettre, Contact angle hysteresis I. Study of an idealized rough surface, Adv. Chem. Ser. 43 (1964) 112–135.
[7] R.J. Good, Contact angle, wetting and adhesion: a critical review, in: K.L. Mittal (Ed.), Contact Angle, Wettability and Adhesion, Festschrift in Honor of Professor Robert J. Good, Utrecht, 1993, pp. 3–36.
[8] R.N. Wenzel, Resistance of solid surfaces to wetting by water, Ind. Eng. Chem. 28 (8) (1936) 988–994.
[9] A.B.D. Cassie, S. Baxter, Wettability of porous surfaces, Trans. Faraday Soc. 40 (1944) 546–551.
[10] S.C.S. Lai, Physical basis and artificial synthesis of the lotus effect Universiteit Leiden, 0020370, Leiden, 2003.
[11] D. Rogers, J. Aprea, T. Bittner, Experimental Design Concept for a Microgravity Whole Body Cleasing System, International Space University Report, France, 2005.
[12] A. Duparre, M. Flemming, G. Notni, Lotus Effect, Kohlrabi Leaf, Motheye, Nanostructure Design for Ultra-hydrophobic Surfaces, 2004, http://www.iof.fhg.de/pr/scientific-annual/_media/2004/a_duparre.pdf (Accessed 15 July 2004).
[13] I. Luzinov, P. Brown, G. Chumanov, S. Minko, Ultrahydrophobic Fibers: Lotus Approach, National Textile Center, 2004 (Project No:C04-CL06).
[14] W. Barthlott, C. Neinhuis, Purity of sacred lotus, or escape from contamination in biological surfaces, Planta 202 (1997) 1–8.
[15] D.M. Anderson, Chief Lexicographer, Dorland's Illustrated Medical Dictionary, 32nd ed., Elsevier Saunders, Philadelphia, PA, 2010, pp. 11–17.
[16] B. Higgs, W. White, Solid Antimicrobial, U.S. Pat. 5359104, 1994.
[17] A.J. Isquith, E.A. Abbott, P.A. Walters, Surface-bonded antimicrobial activity of an organosilicon quaternary ammonium chloride, Appl. Microbiol. 24 (6) (1972) 859–863.
[18] S. Ozcan, N. Calis Acikbas, G. Acikbas, Formation of antibacterial effect on ceramic tile surfaces, Anadolu Univ. J. Sci. Technol. A – Appl. Sci. Eng. 18 (1) (2017) 122–130.
[19] S.A. Onaizi, S.S.J. Leong, Tethering antimicrobial peptides, Biotechnol. Adv. 29 (2011) 67–74.
[20] G. Acikbas, Micromorphology Formation on Ceramic Surfaces, Master's Thesis, Anadolu University, Eskişehir, Turkey, 2007.
[21] C. Neinhuis, W. Barthlott, Characterization and distribution of water-repellent, self-cleaning plant surfaces, Ann. Bot. 79 (1997) 667–677.
[22] E.H. Ishida, Channelling the forces of nature – human and earth conscious materials may create new waves, Qualicer 1 (2004) 1–23.
[23] S. Ashokkumar, J. Adler-Nissen, P. Moller, Factors affecting the wettability of different surface materials with vegetable oil at high temperatures and its relation to cleanability, Appl. Surf. Sci. 263 (2012) 86–94.
[24] X. Chen, Y.G.X. Suo, J. Huang, Y. Liu, H. Li, Construction of mechanically durable superhydrophobic surfaces by thermal spray deposition and further surface modification, Appl. Surf. Sci. 356 (2015) 639–644.
[25] B.S. Yilbas, M. Khaled, N. Abu-Dheir, N. Aqeeli, S.Z. Furquan, Laser texturing of alumina surface for improved hydrophobicity, Appl. Surf. Sci. 286 (2013) 161–170.
[26] Y. Jia, R. Yue, G. Liu, J. Yang, Y. Ni, X. Wu, Y. Chen, Facile fabrication of nano-structured silica hybrid film with superhydrophobicity by one-step VAFS approach, Appl. Surf. Sci. 265 (2013) 405–411.
[27] M. Piispanen, L. Hupa, Comparison of self-cleaning properties of three titania coatings on float glass, Appl. Surf. Sci. 258 (2011) 1126–1131.
[28] A. Sirelkhatim, S. Mahmud, A. Seeni, N.H.M. Kaus, L.C. Ann, S.K.M. Bakhori, H. Hasan, D. Mohamad, Rewiew on zinc oxide nanoparticles: antibacterial activity and toxicity mechanism, Nano-Micro Lett. 7 (3) (2015) 219–242.
[29] J. Pasquet, Y. Chevalier, E. Couval, D. Bouvier, G. Noizet, C. Morliere, M.-A. Bolzinger, Antimicrobial activity of zinc oxide particles on five micro-organisms of the Challenge Tests related to their physicochemical properties, Int. J. Pharm. 460 (2014) 92–100.
[30] J. Pasquet, Y. Chevalier, J. Pelletier, E. Couval, D. Bouvier, M.-A. Bolzinger, The contribution of zinc ions to the antimicrobial activity of zinc oxide, Colloids Surf. A: Physicochem. Eng. Aspects 457 (2014) 263–274.
[31] Y. Xie, Y. He, P.L. Irwin, T. Jin, X. Shi, Antimicrobial activity and mechanism of zinc oxide nanoparticles against *Campylobacter jejuni*, Appl. Environ. Microbiol. 77 (2011) 2325–2331.
[32] F.M. Fowkes, Attractive forces at interfaces, Ind. Eng. Chem. 56 (1964) 40–52.
[33] D. Owens, R. Wendt, Estimation of the surface free energy of polymers, J. Appl. Polym. Sci. 13 (1969) 1741–1747.
[34] D.H. Kaelble, Dispersion-polar surface tension properties of organic solids, J. Adhes. 2 (1970) 66–81.
[35] C. Rulison, Two-Component Surface Energy Characterization As a Predictor of Wettability and Dispersability, AN213, Kruss GmbH, Hamburg, www.kruss.de, 01/2000.
[36] S. Banerjee, Simple derivation of Young, Wenzel and Cassie-Baxter equations and its interpretations, arXiv:0808.1460v1 [cond-mat.mtrl-sci], 11 Aug 2008.
[37] F. Hejda, P. Solar, J. Kousal, Surface free energy determination by contact angle measurements – a comparison of various approaches, WDS'10 Proceedings of Contributed Papers, Part III (2010) 25–30.
[38] Author: FT, Practical Contact Angle Measurement (5), Kruss Technical Note: TN315e, Kruss GmbH, Hamburg, www.kruss.de, 12/2008.
[39] C. Rulison, Models for Surface Free Energy Calculation, Kruss Technical Note: TN306e, Kruss GmbH, Hamburg, www.kruss.de, 06/1999.
[40] C.J. van Oss, Interfacial Forces in Aqueous Media, Marcel Dekker, New York, 1994.

APPLIED SURFACE SCIENCE İNDE | Applied Surface Science - Journa

journals.elsevier.com/applied-surface-science

ELSEVIER

SEARCH MENU

Home › Journals › Applied Surface Science

ISSN: 0169-4332

Applied Surface Science

A Journal Devoted to Applied Physics and Chemistry of Surfaces and Interfaces

Editor-in-Chief: H. Rudolph, PhD

› View Editorial Board

› **CiteScore: 8.7** ⓘ **Impact Factor: 6.182** ⓘ

Submit Your Paper

Supports Open Access

View Articles

Guide for Authors

Abstracting/ Indexing

Track Your Paper

› Elsevier Physics homepage

Applied Surface Science covers topics contributing to a better understanding of **surfaces**, **interfaces**, **nanostructures** and their applications. The journal is concerned with scientific research on the atomic and molecular level of **material properties** determined with **specific surface** analytical techniques...

Read more

Most Downloaded | Recent Articles | Most Cited | Open Access Articles

Resolving surface chemical states in XPS analysis of first row transition metals, oxides and hydroxides: Cr, Mn, Fe, Co and Ni

Mark C. Biesinger | Brad P. Payne | ...

Analysis of XPS spectra of Fe2+ and Fe3+ ions in oxide materials

www.journals.elsevier.com bekleniyor...

TR 21:59 09.11.2020

APPLIED SURFACE SCIENCE INDE | Abstracting Indexing - Applied S

elsevier.com/journals/applied-surface-science/0169-4332/abstracting-indexing

ELSEVIER

About Elsevier | Products & Solutions | Services | Shop & Discover | Search

Visit journal homepage >

Submit your paper >

Open access options >

Guide for authors >

Track your paper >

Order journal >

View articles >

Editorial board >

Abstracting and Indexing

- Aluminium Industry Abstracts
- El Compendex Plus
- INSPEC
- Engineered Materials Abstracts
- Engineering Index
- Metals Abstracts
- Chemical Abstracts
- Current Contents - Physical, Chemical & Earth Sciences
- Current Contents - Engineering, Computing & Technology
- Scopus
- Science Citation Index

TR 22:00 09.11.2020

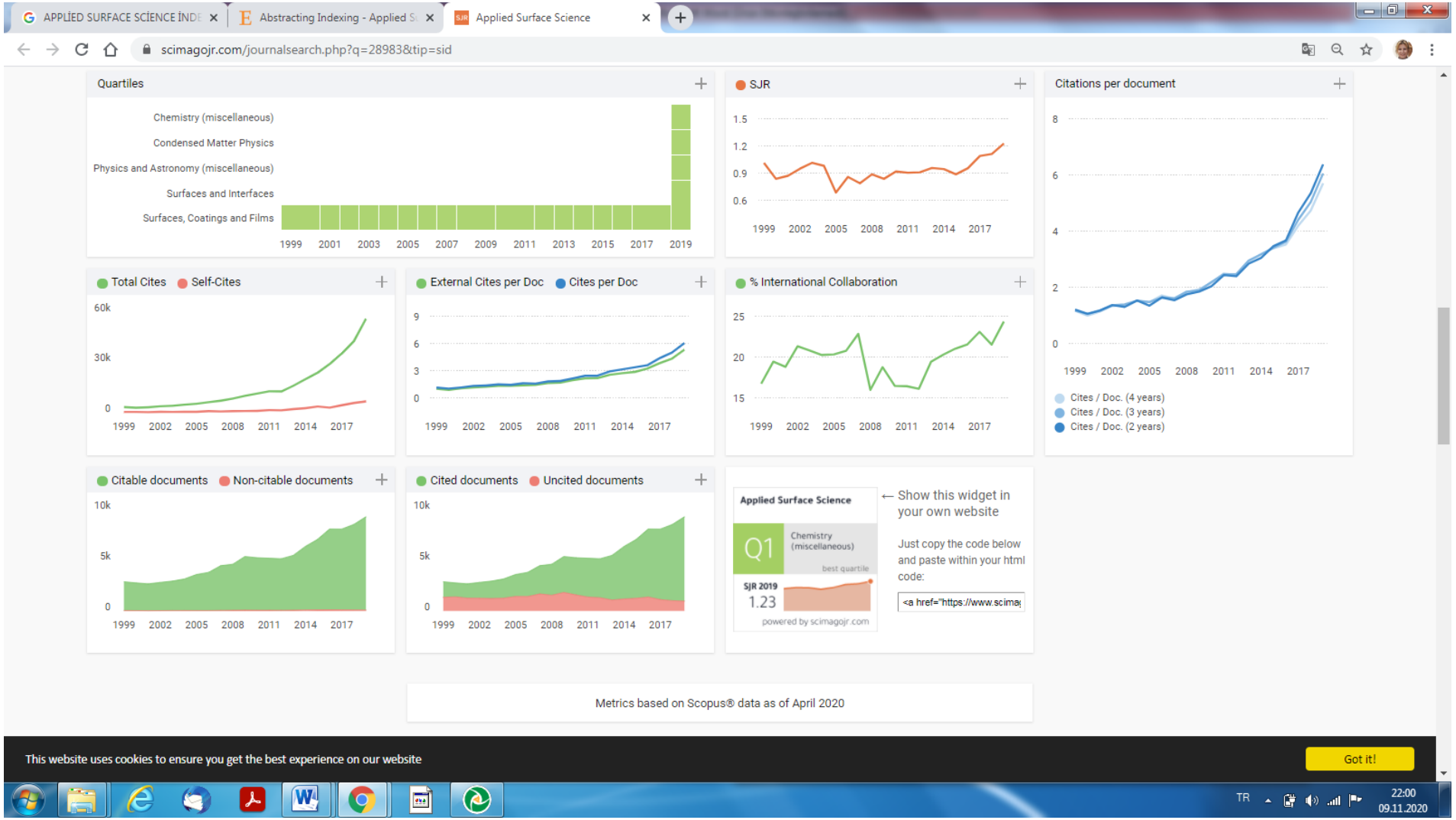
APPLIED SURFACE SCIENCE İNDE
Abstracting Indexing - Applied S
Applied Surface Science
scimagojr.com/journalsearch.php?q=28983&tip=sid
Quartiles
Chemistry (miscellaneous)
Condensed Matter Physics
Physics and Astronomy (miscellaneous)
Surfaces and Interfaces
Surfaces, Coatings and Films
1999 2001 2003 2005 2007 2009 2011 2013 2015 2017 2019
SJR
1.5
1.2
0.9
0.6
1999 2002 2005 2008 2011 2014 2017
Citations per document
8
6
4
2
0
1999 2002 2005 2008 2011 2014 2017
Cites / Doc. (4 years)
Cites / Doc. (3 years)
Cites / Doc. (2 years)
Total Cites
Self-Cites
60k
30k
0
1999 2002 2005 2008 2011 2014 2017
External Cites per Doc
Cites per Doc
9
6
3
0
1999 2002 2005 2008 2011 2014 2017
% International Collaboration
25
20
15
1999 2002 2005 2008 2011 2014 2017
Citable documents
Non-citable documents
10k
5k
0
1999 2002 2005 2008 2011 2014 2017
Cited documents
Uncited documents
10k
5k
0
1999 2002 2005 2008 2011 2014 2017
Applied Surface Science
Q1
Chemistry (miscellaneous)
best quartile
SJR 2019
1.23
powered by scimagojr.com
Show this widget in your own website
Just copy the code below and paste within your html code:
<a href="https://www.scima
Metrics based on Scopus® data as of April 2020
This website uses cookies to ensure you get the best experience on our website
Got it!
TR
22:00
09.11.2020